Journal of Materials Chemistry A

Accepted Manuscript

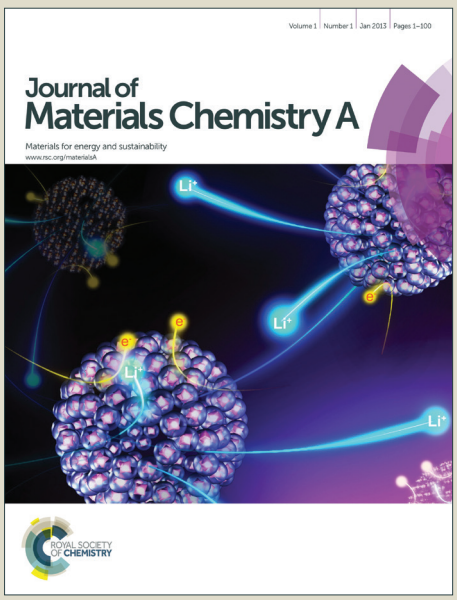

ROYAL SOCIETY OF CHEMISTRY

www.rsc.org/materialsA

Cite this: DOI: 10.1039/c0xx00000x

www.rsc.org/xxxxxx

ARTICLE TYPE

Ruthenium(II) Quasi-Solid State Dye Sensitized Solar Cells with 8% Efficiency using Supramolecular Oligomer-Based Electrolyte

K. L. Vincent Joseph,[a] A. Anthonysamy,[a] P. Sudhagar,[b] Woohyung Cho,[b] Young Soo Kwon,[c] Taiho Park,[c] Yong Soo Kang[b] and Jin Kon Kim[a,*]

Received (in XXX, XXX) Xth XXXXXXXXX 20XX, Accepted Xth XXXXXXXXX 20XX
DOI: 10.1039/b000000x

We have achieved 8% efficiency for the Ruthenium(II) dye, **SY-04**, in quasi-solid state dye sensitized solar cells using supramolecular oligomer-based electrolyte. The dyes in this study, **SY-04** and **SY-05,** which were synthesized through highly efficient synthetic routes, showed better molar extinction coefficients compared to that of the **Z907** dye. In the absorption spectra, **SY-04** and **SY-05** displayed better red shifted metal ligand charge transfer (MLCT) absorption bands at 533, 382 and 535, 373 nm, respectively, compared with 521, 371 nm of **Z907** dye. Also, **SY-04** and **SY-05** showed better molar extinction coefficients, 6691, 16189 M^{-1} cm^{-1} and 6694, 16195 M^{-1} cm^{-1} as compared with **Z907** dye, 4308, 4917 M^{-1} cm^{-1}. When excited into the charge-transfer absorption band of **SY-04** and **SY-05** in ethanol at 77 K, broad emission band for **SY-04** and **SY-05** with a maximum at 788 nm and 786 nm, respectively, was observed compared to the emission band of **Z907** at 797 nm. The current-voltage characteristics of the **SY-04** sensitizer gave the best performance data, J_{SC} = 18.0 mA cm^{-2}, V_{OC} = 0.662 V, *ff* = 0.663, and η of 8.0 %. The increased V_{OC} value for **SY-04** than **Z907** is mainly attributed to high charge recombination resistance by effective dye coverage, which is confirmed by impedance spectroscopy.

Introduction

The dye-sensitized solar cell (DSC) has emerged as one of the most promising alternatives to cost-intensive silicon-based photovoltaic devices.[1] The conventional DSC is composed of two conductive substrates, porous structured metal oxide semiconductor film coated with a sensitizer and a liquid electrolyte. Although power conversion efficiencies (PCEs) of close to 13% could be achieved with this device architecture,[2, 3] the existence of the liquid electrolyte in DSCs has several drawbacks such as leakage, volatilization of organic solvent, possible desorption of the surface-coated dyes, corrosion of the counter electrodes and limited long-term performance, which restricts the widespread commercialization of DSCs.[4] Replacing liquid electrolytes with hole-transporting materials (HTMs) is one of the most promising methods to avoid these problems.[5] Several attempts, such as organic hole conductors,[6, 7] physically cross-linked gelators,[8, 9] and polymer gel electrolytes,[10] have been applied as alternatives to liquid electrolytes. Therefore, research on solid state or quasi-solid state dye sensitized solar cells (sDSCs), based on polymer electrolytes has become attractive.[4, 8, 11-17]

However, compared with liquid electrolytes, solid state electrolytes often show relatively lower ionic conductivity and poor electrolyte/electrode interfacial contact.[5] Among the solid/semi-solid electrolytes studied so far, polymer based quasi-solid-state electrolytes have been attracting a great deal of interest for their good contact with nano-crystalline TiO_2 electrodes and counter electrodes, maintaining good ionic conductivity, reducing cell leakage problems and their comparable efficiencies to cells using liquid electrolytes.[18, 19] Polymers or co-polymers, such as poly(ethylene oxide) (PEO),[18] poly(styrene-co-acrylonitrile),[20] poly(ethylene glycol) (PEG),[19] poly(methylmethacrylate) (PMMA),[21] poly-(acrylonitrile-co-vinyl acetate)[22] and poly(vinylidene fluoride-co-hexafluoropropylene)[23, 24] have been applied as the gel electrolytes.

Oligomers have been utilized successfully by a technique known as the "oligomer approach" to provide better interfacial contact between dyes and electrolytes as well as increased ionic conductivity for sDSCs, resulting in high-energy conversion efficiencies.[13-15] Three different oligomer approaches for the preparation of sDSCs employing liquid oligomer-based electrolytes have been reported. The first approach was to utilize supramolecules of PEG oligomer (Mw 1000 g/mol), which is a liquid during the cell fabrication procedure but becomes a solid polymer electrolyte upon solvent evaporation. This solidification

[a] *Creative Research Initiatives Centre for Smart Block Copolymer Self-Assembly and [c] Polymer Chemistry and Electronics Laboratory, Department of Chemical Engineering, Pohang University of Science and Technology, Pohang, Hyungbuk, 790-784, Republic of Korea.*
[b] *WCU Program Department of Energy Engineering, Hanyang University, Seoul, 133-791, Republic of Korea.*
**E-Mail: jkkim@postech.ac.kr*
DOI: 10.1039/b000000x/

is referred to as *in situ* self-solidification, and energy conversion efficiency (η) of 3.34% was achieved.[13] Second, the use of an oligomer blend containing an amorphous liquid oligomer poly(propylene glycol) (Mw = 750 g/mol) with high-molecular-weight PEO (Mw = 1,000,000 g/mol) resulted in an η of 3.84%.[14] Third, low molecular poly(ethylene glycol) oligomer (Mw = 500 g/mol) based electrolytes have been solidified using fumed silica nanoparticles as a networking agent to become nanocomposites, resulting in a comparably good conversion efficiency of 4.5%.[15] Therefore, the oligomer approach utilizing liquid oligomers, followed by *in situ* self-solidification has proven to be very effective for preparing sDSCs with good energy conversion efficiency, primarily resulting from the enlarged interfacial contact between the dyes and the electrolyte and the increased ion conductivity.[25]

sDSCs with high efficiency have been reported when using an amphiphilic, heterolyptic ruthenium sensitizer.[26-28] This improved efficiency is attributed to the self-assembly of the dye, which forms a dense layer on the surface of the TiO_2 nanoparticles, with its carboxylate group acting as anchors and its hydrophobic isolating chains acting as a blocking layer between the hole conductor and the TiO_2.[26-28] sDSCs are particularly interesting, with their open circuit photovoltage (V_{OC}) often exceeding that of electrolyte-based DSCs due to a smaller energy loss during the dye regeneration process.[29, 30] Nevertheless, the overall photovoltaic conversion efficiency of sDSCs attained currently with standard ruthenium complexes[28] or organic dyes[31] remains significantly below that of electrolyte-based devices because the short-circuit current (J_{SC}) of the former is about smaller compared to the latter. The smaller J_{SC} values in the case of ruthenium complexes arise from the fact that the sDSCs usually employ only 1.5 to 3-μm-thick nanocrystalline TiO_2 films to ascertain quantitative collection of the photo-generated charge carriers and complete pore filling by the hole conductor. As the solar light harvesting by such thin films depends strongly on the optical cross section of the sensitizer, the use of a high-molar-extinction-coefficient dye in combination with such thin mesoporous TiO_2 electrodes is advantageous. Much research has focused on increasing the extinction coefficient and red response of heterolyptic ruthenium complexes by extending the π-conjugation of the ancillary ligand and endowing it with electron-donating groups.[6, 26, 32-35]

In solid state electrolyte-based DSSCs the electrolyte percolation throughout the photoanode pore-channel governs with thickness of the photoanode (TiO_2), pore diameter and dye structure. Unlike liquid electrolyte-based DSSCs, the high thickness TiO_2 electrode exhibits poor filling for solid state electrolyte. Therefore, a small thickness electrode is always desirable for effective pore-filling. But, the small thickness electrode has a disadvantage on light harvesting. To balance the electrolyte pore-filling and effective light harvesting even for small thickness of TiO_2 electrode, one should find high-molar-extinction-coefficient-dye.

In this work, we utilized supramolecular oligomer based polymer electrolytes to ensure effective pore filling for the preparation of quasi-sDSCs based on ruthenium dyes with high molar extinction coefficient. We have previously reported that **SY-04** and **SY-05** dyes prepared through the efficient HEW reaction showed high molar extinction coefficient. When we fabricated quasi-sDSC based on **SY-04**, it showed a maximum power conversion efficiency of 8.0%, which is a 10% increase compared with that of quasi-sDSC based on **Z907** at the same fabrication condition.

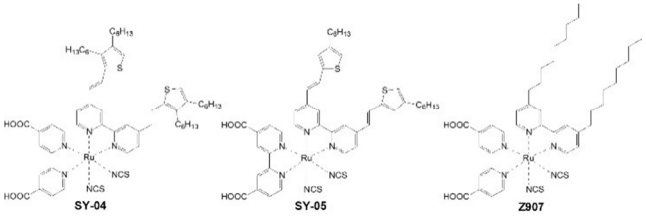

Fig. 1 Molecular structures **SY-04**, **SY-05** and **Z907**.

Experimental Section

General Procedures. All of the reactions were performed under nitrogen atmosphere, and solvents were distilled from appropriate drying agents prior to use. Commercially available reagents were used without further purification, unless otherwise stated. All reactions were monitored using precoated thin-layer chromatography plates (0.20 mm) with fluorescent indicator UV254 (uvitec-LF-204.LS). The organic precursors were purified by column chromatography using Silica gel (60-120 mesh, Merck). The complexes, **SY-04** and **SY-05** were purified using Sephadex-LH-20 (Sigma) resin. ^1H and ^{13}C NMR spectra were recorded on a Bruker AMX 500 or AV 500 instrument. Mass spectra were obtained on a JMS-700 double focusing mass spectrometer (JEOL, Tokyo, Japan). Elemental analysis was carried out with a Perkin-Elmer 2400 CHN analyzer. Electronic absorption spectra were obtained on a Cary 50 Probe UV–visible-NIR spectrophotometer. The cyclic voltammograms were recorded on a CHI600A electrochemical analyzer.

Synthesis of SY-04 and SY-05. The ruthenium dyes, **SY-04** and **SY-05** were synthesized previously and the molecular structures are given in Figure 1.[36]

Electrolyte Preparation. The oligomer blend electrolyte was made by blending the high-molecular-weight PEO (Mw 1,000,000 g/mol) and low-molecular-weight poly(ethylene glycol) dimethyl ether, (oligo-PEGDME, Mw 500 g/mol) with a mole ratio of [-O-]/[XI]) 20:1 (here X is, 1-methyl-3-propylimidazolium cation) and XI/I_2, 10:1, w/w in acetonitrile. The blend ratio of PEO to the oligomer was fixed at 4:6 (w/w). The advantage of using MPII (1-methyl-3-propylimidazolium iodide) is that it is an ionic liquid that does not exhibit any vapour pressure issue. All chemicals were purchased from Aldrich and used as received. MPII was obtained from Solaronix (Switzerland).[13-15]

DSC Fabrication. Quasi-sDSCs were fabricated as follows. Transparent SnO_2/F-layered conductive glass (FTO, purchased from Pilkington. Co. Ltd., Pilkington-TEC8) was employed to prepare both the photo- and counter-electrodes. For the photoelectrode, a $TiCl_4$ solution (Aldrich) was first spin-coated onto FTO glass, and then the glass was heated stepwise to 450 °C and maintained at this temperature for 20 min. Commercialized TiO_2 paste of 20 nm size (Ti-Nanoxide T, Solaronix) was cast onto the FTO glass by a doctor-blade technique and successive

sintering at 450 °C for 30 min. The nanocrystalline TiO_2 film (with a thickness of *ca.* 13-18 μm) was sensitized overnight with **SY-04**, **SY-05** and **Z907** (Ruthenizer 520-DN, Solaronix) dye solutions. Pt-layered counter-electrodes were prepared by spin-coating of an H_2PtCl_6 solution (0.05 mol dm^{-3} in isopropanol, Aldrich) onto FTO glass and then successive sintering at 400 °C for 30 min. For solar cell fabrication, a dilute polymer electrolyte solution was first cast onto a dye-adsorbed TiO_2 electrode and evaporated very slowly for easy penetration of electrolytes through the nanopores of the TiO_2 layer. Next, a highly concentrated polymer electrolyte solution was cast onto the photoelectrode to minimize the time for evaporation of solvent as well as to prevent the formation of cavities between the two electrodes during the solvent evaporation. Both electrodes were superposed together and then pressed between two glass plates to achieve slow evaporation of solvent as well as to obtain a very thin SPE layer. The cells were placed in a vacuum oven for the complete evaporation of solvent for 1 day and then sealed with an epoxy resin.

Current Voltage Measurements. *J-V* curves were measured with a solar simulator (Newport, Oriel Class A, 91195A) with a source meter (Keithley 2420) at 100 mA cm^{-2} illumination (AM 1.5G) and a calibrated Si reference cell certified by NREL.

Incident Photon-to-Current Conversion Efficiency Spectra (IPCE). IPCE spectra were measured using a power source with a monochromator (Zahner GmbH) and a multimeter (Keithley 2001). Frequency of 5Hz and less than 10 % of amplitude was applied during the measurement.

Electrochemical Impedance Spectra (EIS). EIS spectra were measured with a computer-controlled potentiostat (SP-200, BioLogic, France) producing a small amplitude harmonic voltage, and a frequency response analyzer module. The EIS experiments were performed under dark conditions. The impedance spectra of the devices were obtained at various potentials at 0.62 V for **Z907** and 0.57 V for **SY-04**, **SY-05** at frequencies ranging from 0.05 Hz to 1 MHz, the oscillation potential amplitudes having *ca*. 25 mV. The measured spectra were fit to an appropriate simplified circuit using the Z-fit software provided by BioLogic (EC-Lab).

Results and Discussion

Photophysical Studies

The absorption and emission spectra for **SY-04**, **SY-05** and **Z907** dyes measured in ethanol (EtOH) are shown in Figure 2, and the selected parameters are summarized in Table 1. In the UV region, **SY-04** and **SY-05** dyes show intense absorption bands at 311 nm and 314 nm, which are assigned to the ligand-centred π-π* transitions of the dihexyl thiophene ancillary ligand and dcbpy. These transitions have better molar extinction coefficients (ε), (17088, 16209 M^{-1} cm^{-1}), compared to that of **Z907** dye (15506 M^{-1} cm^{-1}). In the visible region, **SY-04** and **SY-05** show better red shifted MLCT absorption bands at 533, 382 and 535, 373 nm compared with 521, 371 nm for **Z907** dye. In this region also, **SY-04** and **SY-05** show better molar extinction coefficients, 6691, 16189 M^{-1} cm^{-1} and 6694, 16195 M^{-1} cm^{-1} as compared with **Z907** dye (4308, 4917 M^{-1} cm^{-1}). The enhanced molar extinction coefficients and the red shifts are attributed to the extension of π-conjugation in both **SY-04** and **SY-05** dyes. The red shift of the MLCT band suggests that the band gap between the HOMO and LUMO levels for **SY-04** and **SY-05** becomes smaller than that of **Z907**. All the dyes show low emission bands. When excited into the charge-transfer absorption band of **SY-04** and **SY-05** in EtOH at 77 K, there was a broad emission band with a maximum at 788 nm for **SY-05**, which is attributed to the luminescence from the lowest energy MLCT state of **SY-04** and **SY-05** dyes. **Z907** shows a luminescent band at 797 nm. The

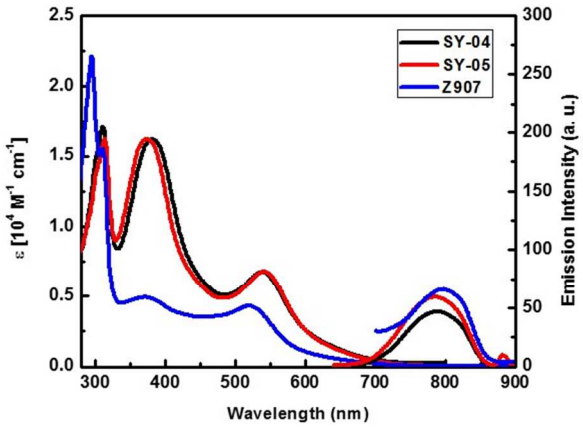

emission spectra of **SY-04**, **SY-05** and **Z907** are shown in Figure 2.

Fig. 2 Absorption spectra of **SY-04**, **SY-05** and **Z907** in EtOH.

Electrochemical Studies

All of the oxidation and reduction potentials of **SY-04**, **SY-05** and **Z907** were measured in DMF with 0.1 M $TBAPF_6$ (vs natural hydrogen electrode (NHE)). It was calibrated with ferrocene/ferrocenium as the reference and converted to NHE by addition of 0.47 V.[36, 37] As shown in Table 1, the electrochemical oxidation potentials, $E°_{ox}$, of **SY-04** and **SY-05** are in the range 0.88 to 0.92 V vs NHE that are more compared to **Z907** (0.836 V), which is larger than that of the I^-/I_3^- redox couple (*ca.* 0.4 V vs NHE). The excited-state oxidation potentials, $E°_{ox}$*, which range from -0.91 to -0.95 V and -1.04 for **Z907**, are sufficiently more negative than the conduction-band edge of the TiO_2 electrode (*ca.* −0.5 V vs NHE). The LUMO levels of **SY-04** (−3.38 eV) and **SY-05** (−3.42 eV) are more negative compared to the LUMO levels of **Z907** (−3.28 eV). This ensures that there is enough driving energy for **SY-04** and **SY-05** dyes for dye regeneration to occur as compared to **Z907,** and also verifies that the excited-state oxidation potentials, $E°_{ox}$*, are more negative than the conduction band of TiO_2 for efficient electron injection.

Photovoltaic Studies

The *J-V* curves of the quasi-sDSCs using **SY-04**, **SY-05** and **Z907** sensitizers are presented in Figure 3. The measurements were carried out at AM 1.5G (100 $mWcm^{-2}$ photon flux), and the photovoltaic parameters of the cells are listed in Table 2. The **SY-04** dye based quasi-sDSCs yielded markedly higher open-circuit potential, V_{OC} = 0.662 V, fill factor, *ff* = 0.663 than that of **SY-05**

and **Z907** dyes.

Table 1 Photophysical and electrochemical properties of **SY-04**, **SY-05** and **Z907**.

Dye	λ_{abs} (nm) (ε, M^{-1} cm^{-1})[a]	λ_{em} (nm)[b]	$E_{0\text{-}0}$ (eV)[c]	E^0_{ox} (V)[d]	E_{HOMO} (eV)[e]	E_{LUMO} (eV)[f]	E^0_{ox}* (eV)[g]
SY-04	533 (6691), 382 (16189), 311 (17088)	788	1.83	0.88	-5.21	-3.38	-0.95
SY-05	535 (6695), 373 (16195), 314 (16209)	786	1.83	0.92	-5.25	-3.42	-0.91
Z907	521 (4309), 371 (4917), 295 (22161)	797	1.88	0.836	-5.16	-3.28	-1.04

[a] The absorption spectrum was measured in EtOH. [b] The emission spectrum was recorded in EtOH at 77 K. [c] $E_{0\text{-}0}$ was determined from the intersection of the absorption and tangent of the emission peak in EtOH ($E_{0\text{-}0}$ = 1240/λ_{max}). [d] The oxidation and reduction potentials (vs. NHE) were measured in DMF with 0.1 M (n-Bu_4N)PF_6 and at a scan rate of 20 mVs^{-1}. It was calibrated with Fc/Fc+ and converted to the NHE scale by addition of 0.47 V. [e] E_{HOMO} was calculated as -4.8 - (E^o_{ox} - $E_{1/2}$ of Fc/Fc^+), where $E_{1/2}$ of Fc/Fc^+ = -0.47 V. [f] E_{LUMO} was calculated as E_{HOMO} + $E_{0\text{-}0}$. [g] $E°_{ox}$* was calculated as $E°_{ox}$ - $E_{0\text{-}0}$.

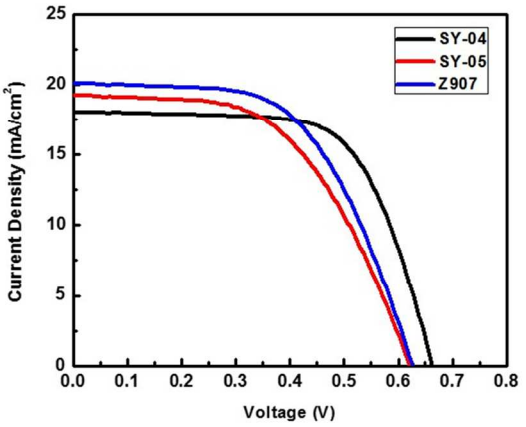

Fig. 3 *J-V* curves of quasi-sDSCs based on **SY-04**, **SY-05** and **Z907**.

Table 2 Performance of quasi-sDSCs Measured under AM 1.5G One-Sun Irradiation.

Dye	J_{SC} (mA cm^{-2})	V_{OC} (mV)	*ff* (%)	η (%)	TiO_2 Thickness (μm)[a]
SY-04	18.0	662.3	66.3	8.0	6+4
SY-05	19.3	620.1	53.7	6.4	6+4
Z907	20.1	626.1	57	7.2	6+4

[a] 400 nm size TiO_2 anatase scattering layer. The active areas of the cells were 0.16 cm^{-2}.

This implies that the high PCE, η = 8%, in **SY-04** device originates from high V_{OC} of the device. The high V_{OC} in DSC may be ascribed to several reasons: (a) effective coverage of dye molecules on TiO_2 surface, possibly retarding the recombination pathways of electron leakage from TiO_2 to electrolyte,[38,39] (b) increased difference in Fermi level between photoanode and electrolyte redox, and (c) the efficient charge transfer characteristic at dye/electrolyte interface.[40] In general, V_{OC} of a device depends on the Fermi level difference between TiO_2 and redox position of the electrolyte. The energy level position of dye is not directly participating in determining the V_{OC} of the device. However, the dye-regeneration rate influences the V_{OC} of the device. For instance, a large difference between the HOMO level and redox will take larger redox shuttle distance for supplying electron to dye. This results in weak dye regeneration and affects the electron injection from dye to TiO_2. It is clear that poor electron injection at TiO_2 Fermi level shows small difference between redox mediator and TiO_2 Fermi level, consequently, lowering the V_{OC} value. Therefore, the HOMO of a dye[36] influences the V_{OC} of the device through controlling dye-regeneration.[41] The high photocurrent existence in **SY-05** compared to **SY-04** may be attributed to the difference in light photon reception in the visible light wavelengths. The higher fill factor of the **SY-04** may be attributed to the presence of two alkyl chains on the thiophene moiety, which increases the solubility of the dye and reduces aggregation and exhibits good compatibility. The above discussion indicates that **SY-04** sensitizer is effective with solid-state electrolyte, and shows 8% higher performance than that (η = 7.2%) of the quasi-sDSC cell based on **Z907** under the same cell fabrication conditions.

IPCE

To understand high photocurrent generations by **SY-05** and **Z907** compared with **SY-04**, the photocurrent generation at different wavelengths have been evaluated, and the results are given in Figure 4. **SY** sensitizers achieved the maximum in the 480-580 nm range, due to the presence of MLCT absorption bands in that region with the onset value of 800 nm. **Z907** showed the maximum of 87% at 529 nm, which is responsible for the highest J_{SC} value of 20.1 mA cm^{-2} as compared to the **SY**-sensitizers. The **SY-05** dye exhibited its maximum IPCE at 529 nm and showed a broad visible light harvesting region compared to **SY-04**. This corroborates that the possibility of red photon light harvesting in **SY-05** which drives higher photocurrent generation compared to **SY-04**. These results are consistent with Table 2. The mismatch between UV-visible spectra and IPCE of the dyes is due to the loss of photocurrent[42] and the scattering of the incident light by the FTO glass.[43]

Impedance

As discussed earlier, effective dye anchoring on TiO_2 surface could promote the charge recombination resistance at TiO_2/dye interfaces and is further analyzed by electrochemical impedance spectroscopy.[44-46] The Nyquist plots of quasi-sDSCs using

different dye sensitizers are presented in Figure 5. The second frequency semicircle in the Nyquist plot represents the charge transfer phenomena between the TiO_2 surface and the electrolyte. Under dark condition, the diameter of the second semicircle refers to the charge recombination resistance (R_{re}) of TiO_2/electrolyte interfaces, i.e., dark current.[47, 48] From the equivalent circuit analysis, **SY-04** sensitizer showed higher R_e~103.8 Ω than **SY-05** (R_e~80.5 Ω) indicating that a large amount of C_6H_{13} moieties (dye forest) at **SY-04** dye is effectively blocking the direct contact between TiO_2 surface and electrolyte, thus retarding the undesirable electron leakage from TiO_2 to electrolyte. The reduced recombination pathways at TiO_2/**SY-04**/electrolyte interfaces shifting more negative TiO_2 Fermi level position result in high V_{OC} in this system. Comparatively, the fact that **Z907** showed high R_e value 112.9 Ω to **SY** sensitizers may arise from the effective dye coverage at TiO_2 surface.

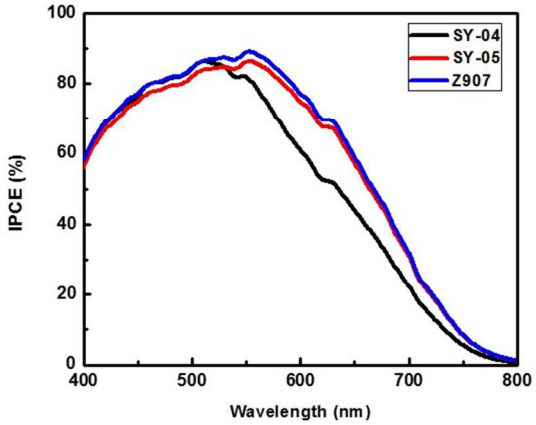

Fig. 4 IPCE spectra of **SY-04, SY-05** and **Z907**.

Nevertheless, **Z907** dye showed less V_{OC} than **SY-04**. One possible reason for the contradictory V_{OC} reduction may originate from less electron lifetime. Thus, we analyzed the Bode phase characteristic plots of quasi-sDSCs. The **SY-04** sensitizer-based device exhibited a large shift towards lower frequency, revealing an increase in the apparent recombination lifetime. The estimated high electron life time τ ~ 54.7 ms (calculated as, $\tau = 1/\omega^*$, in which ω* is the frequency at the maximum peak in Figure 6) at **SY-04** compared to other devices fostered high V_{OC} in this system and is in agreement with results given in Table 2. Furthermore, the decrease in the V_{OC} of the **SY-05** dye (τ ~ 39.7 ms) also resulted in the decrease in the lifetime as compared to that (τ ~ 44.1 ms) of the **Z907.**

We have also obtained the Bode plots of quasi-sDSCs measured after 10 days of the fabrication at room temperature and the results are shown in Figure 6. After 10 days, sDSC devices based on both **SY-04** and **Z907** dyes show significant shift in the first peak position toward higher frequency region. This implies that either gelator or dye in the electrolyte is slightly modified by the environment or sealing condition. On the other hand, sDSC based on **SY-05** dye does not show any significant change in the first peak position. This suggested that **SY-05** dye is having better compatibility with the gelator in the electrolyte than that of **SY-04** and **Z907** dye.[49]

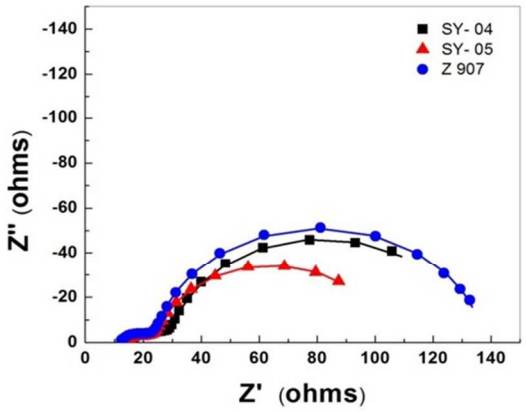

Fig. 5 Nyquist plots of **SY-04**, **SY-05** and **Z907** measured at dark condition. Experimental data is represented by symbols and the solid line corresponds to the fits obtained with Z-View software.

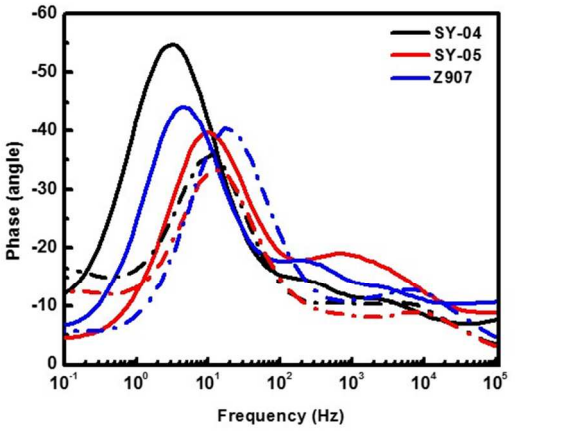

Fig. 6 The bode plots of sDSCs using **SY-04, SY-05 and Z907** measured at dark (solid curves represent the pristine devices and dash curves indicate the measurement of the devices after 10 days at room temperature).

Conclusions

In this study, we have optimized supramolecular oligomer-based electrolytes for high molar extinction coefficient **SY-04** and **SY-05** ruthenium dyes for fabricating quasi-sDSCs. These dyes show good photophysical properties as compared to the **Z907** dye. The electrochemical oxidation potentials, E°_{ox}, of **SY-04** and **SY-05** are more compared to **Z907** and are larger than that of the I^-/I_3^- redox couple. The excited-state oxidation potentials, E°_{ox}*, of **SY-04** and **SY-05** are sufficiently more negative than the conduction-band edge of the TiO_2 electrode. The LUMO levels of **SY-04** and **SY-05** are more negative compared to the LUMO levels of **Z907** and ensure that there is enough driving energy for **SY-04** and **SY-05** dyes for dye regeneration to occur as compared to **Z907**. The **SY-04** based quasi-solid state solar cell achieved a

maximum power conversion efficiency of 8.0%, which is very high as compared to the previously reported sDSCs based on the amphiphilic ruthenium dyes. The IPCE spectra and electrochemical impedance spectra are well consistent with J_{SC} and V_{OC} values of the dyes.

Acknowledgements

This work was supported by the National Creative Research Initiative Program supported by the National Research Foundation of Korea (NRF).

References

1. A. Hagfeldt, G. Boschloo, L. Sun, L. Kloo and H. Pettersson, *Chem. Rev.*, 2010, **110**, 6595-6663.
2. A. Yella, H.-W. Lee, H. N. Tsao, C. Yi, A. K. Chandiran, M. K. Nazeeruddin, E. W.-G. Diau, C.-Y. Yeh, S. M. Zakeeruddin and M. Grätzel, *Science*, 2011, **334**, 629-634.
3. S. Mathew, A. Yella, P. Gao, R. Humphry-Baker, B. F. Curchod, N. Ashari-Astani, I. Tavernelli, U. Rothlisberger, M. K. Nazeeruddin and M. Grätzel, *Nature Chem.*, 2014, **6**, 242-247.
4. A. F. Nogueira, J. R. Durrant and M. A. De Paoli, *Adv. Mater.*, 2001, **13**, 826-830.
5. U. Bach, D. Lupo, P. Comte, J. Moser, F. Weissörtel, J. Salbeck, H. Spreitzer and M. Grätzel, *Nature*, 1998, **395**, 583-585.
6. C. S. Karthikeyan, H. Wietasch and M. Thelakkat, *Adv. Mater.*, 2007, **19**, 1091-1095.
7. P. Docampo, S. Guldin, M. Stefik, P. Tiwana, M. C. Orilall, S. Hüttner, H. Sai, U. Wiesner, U. Steiner and H. J. Snaith, *Adv. Funct. Mater.*, 2010, **20**, 1787-1796.
8. P. Wang, S. M. Zakeeruddin, I. Exnar and M. Grätzel, *Chem. Commun.*, 2002, 2972-2973.
9. Y. Zhou, W. Xiang, S. Chen, S. Fang, X. Zhou, J. Zhang and Y. Lin, *Chem. Commun.*, 2009, 3895-3897.
10. J. Zhao, X. Shen, F. Yan, L. Qiu, S. Lee and B. Sun, *J. Mater. Chem.*, 2011, **21**, 7326-7330.
11. T. Stergiopoulos, I. M. Arabatzis, G. Katsaros and P. Falaras, *Nano Lett.*, 2002, **2**, 1259-1261.
12. G. Katsaros, T. Stergiopoulos, I. Arabatzis, K. Papadokostaki and P. Falaras, *J. Photochem. Photobiol. A: Chem.*, 2002, **149**, 191-198.
13. Y. J. Kim, J. H. Kim, M. S. Kang, M. J. Lee, J. Won, J. C. Lee and Y. S. Kang, *Adv. Mater.*, 2004, **16**, 1753-1757.
14. M.-S. Kang, J. H. Kim, Y. J. Kim, J. Won, N.-G. Park and Y. S. Kang, *Chem. Commun.,* 2005, 889-891.
15. J. H. Kim, M.-S. Kang, Y. J. Kim, J. Won, N.-G. Park and Y. S. Kang, *Chem. Commun.*, 2004, 1662-1663.
16. W. Kubo, T. Kitamura, K. Hanabusa, Y. Wada and S. Yanagida, *Chem. Commun.*, 2002, 374-375.
17. E. Stathatos, P. Lianos, U. Lavrencic-Stangar and B. Orel, *Adv. Mater.*, 2002, **14**, 354.
18. J. N. de Freitas, A. F. Nogueira and M.-A. De Paoli, *J. Mater. Chem.*, 2009, **19**, 5279-5294.
19. J. Wu, S. Hao, Z. Lan, J. Lin, M. Huang, Y. Huang, L. Fang, S. Yin and T. Sato, *Adv. Funct. Mater.*, 2007, **17**, 2645-2652.
20. J. Wu, Z. Lan, D. Wang, S. Hao, J. Lin, Y. Huang, S. Yin and T. Sato, *Electrochim. Acta*, 2006, **51**, 4243-4249.
21. H. Yang, M. Huang, J. Wu, Z. Lan, S. Hao and J. Lin, *Mater. Chem. Phys.*, 2008, **110**, 38-42.
22. C. L. Chen, H. Teng and Y. L. Lee, *Adv. Mater.*, 2011, **23**, 4199-4204.
23. P. Wang, S. M. Zakeeruddin, J. E. Moser, M. K. Nazeeruddin, T. Sekiguchi and M. Grätzel, *Nature Mater.*, 2003, **2**, 402-407.
24. Z. Huo, S. Dai, K. Wang, F. Kong, C. Zhang, X. Pan and X. Fang, *Sol. Energy Mater. Sol. Cells*, 2007, **91**, 1959-1965.
25. M.-S. Kang, J. H. Kim, J. Won and Y. S. Kang, *J. Phys. Chem. C*, 2007, **111**, 5222-5228.
26. J. Krüger, R. Plass, L. Cevey, M. Piccirelli, M. Grätzel and U. Bach, *Appl. Phys. Lett.*, 2001, **79**, 2085.
27. H. J. Snaith, A. J. Moule, C. Klein, K. Meerholz, R. H. Friend and M. Grätzel, *Nano Lett.*, 2007, **7**, 3372-3376.
28. C.-Y. Chen, M. Wang, J.-Y. Li, N. Pootrakulchote, L. Alibabaei, C.-h. Ngoc-le, J.-D. Decoppet, J.-H. Tsai, C. Grätzel and C.-G. Wu, *ACS Nano*, 2009, **3**, 3103-3109.
29. W. C. Sinke and M. M. Wienk, *Nature*, 1998, **395**, 544-545.
30. M. Grätzel, *Nature*, 2001, **414**, 338-344.
31. J. Burschka, A. Dualeh, F. Kessler, E. Baranoff, N.-L. Cevey-Ha, C. Yi, M. K. Nazeeruddin and M. Grätzel, *J. Am. Chem. Soc.*, 2011, **133**, 18042-18045.
32. J. E. Kroeze, N. Hirata, S. Koops, M. K. Nazeeruddin, L. Schmidt-Mende, M. Grätzel and J. R. Durrant, *J. Am. Chem. Soc.*, 2006, **128**, 16376-16383.
33. A. Holt, J. Leger and S. Carter, *Appl. Phys. Lett.*, 2005, **86**, 123503-123504.
34. D. Kuang, C. Klein, S. Ito, J. E. Moser, R. Humphry-Baker, S. M. Zakeeruddin and M. Graetzel, *Adv. Funct. Mater.*, 2007, **17**, 154-160.
35. C. Y. Chen, S. J. Wu, C. G. Wu, J. G. Chen and K. C. Ho, *Angew. Chem.*, 2006, **118**, 5954-5957.
36. A. Anthonysamy, Y. Lee, B. Karunagaran, V. Ganapathy, S.-W. Rhee, S. Karthikeyan, K. Kim, M. Ko, N.-G. Park and M.-J. Ju, *J. Mater. Chem.*, 2011, **21**, 12389-12397.
37. A. Mishra, N. Pootrakulchote, M. Wang, S. J. Moon, S. M. Zakeeruddin, M. Grätzel and P. Bäuerle, *Adv. Funct. Mater.*, 2011, **21**, 963-970.
38. Y.-G. Lee, S. Park, W. Cho, T. Son, P. Sudhagar, J. H. Jung, S. Wooh, K. Char and Y. S. Kang, *J. Phys. Chem. C*, 2012, **116**, 6770-6777.
39. H. An, D. Song, J. Lee, E.-M. Kang, J. Jaworski, J.-M. Kim and Y. S. Kang, *J. Mater. Chem. A*, 2014, **2**, 2250-2255.
40. Q. Wang, S. Ito, M. Grätzel, F. Fabregat-Santiago, I. Mora-Seró, J. Bisquert, T. Bessho and H. Imai, *J. Phys. Chem. B*, 2006, **110**, 25210-25221.
41. J.-H. Yum, E. Baranoff, F. Kessler, T. Moehl, S. Ahmad, T. Bessho, A. Marchioro, E. Ghadiri, J.-E. Moser and C. Yi, *Nature Commun.*, 2012, **3**, 631.
42. J. M. Ball, M. M. Lee, A. Hey and H. J. Snaith, *Energy Environ. Sci.*, 2013, **6**, 1739-1743.
43. Y. S. Kwon, J. Lim, H.-J. Yun, Y.-H. Kim and T. Park, *Energy Environ. Sci.*, 2014, 7, 1454-1460.
44. F. Fabregat-Santiago, J. Bisquert, G. Garcia-Belmonte, G. Boschloo and A. Hagfeldt, *Sol. Energy Mater. Sol. Cells*, 2005, **87**, 117-131.
45. M. Wang, X. Li, H. Lin, P. Pechy, S. M. Zakeeruddin and M. Gratzel, *Dalton Transactions*, 2009, 10015-10020.
46. R. Yeh-Yung Lin, F.-L. Wu, C.-H. Chang, H.-H. Chou, T.-M. Chuang, T.-C. Chu, C.-Y. Hsu, P.-W. Chen, K.-C. Ho, Y.-H. Lo and J. T. Lin, *J. Mater. Chem. A*, 2014, **2**, 3092-3101.
47. F. Fabregat-Santiago, J. Bisquert, E. Palomares, L. Otero, D. Kuang, S. M. Zakeeruddin and M. Grätzel, *The J. Phys. Chem. C*, 2007, **111**, 6550-6560.
48. M. Adachi, K. Noda, R. Tanino, J. Adachi, K. Tsuchiya, Y. Mori and F. Uchida, *Chem. Lett.*, 2011, **40**, 890-892.
49. R. Kern, R. Sastrawan, J. Ferber, R. Stangl and J. Luther, *Electrochim. Acta*, 2002, **47**, 4213-4225.

Ruthenium(II) Quasi-Solid State Dye Sensitized Solar Cells with 8% Efficiency using Supramolecular Oligomer Based Electrolyte

K. L. Vincent Joseph,[a] A. Anthonysamy,[a] P. Sudhagar,[b] Woohyung Cho,[b] Young Soo Kwon,[c] Taiho Park,[c] Yong Soo Kang[b] and Jin Kon Kim[a,*]

"For Table of Contents Use Only"

We have achieved 8% efficiency for the Ruthenium(II) dye, **SY-04**, in solid state dye sensitized solar cells using supramolecular oligomer-based electrolyte. The dyes in this study, **SY-04** and **SY-05,** showed better photophysical and electrochemical properties compared to **Z907** dye. The **SY-04** based quasi-solid state solar cell achieved excellent power conversion efficiency of 8.0%, against **Z907** (7.2%), which is very high as compared to the previously reported sDSCs based on the amphiphilic ruthenium dyes. The IPCE spectra and electrochemical impedance spectra are well consistent with J_{SC} and V_{OC} values of the dyes as compared to that of the **Z907** dye.

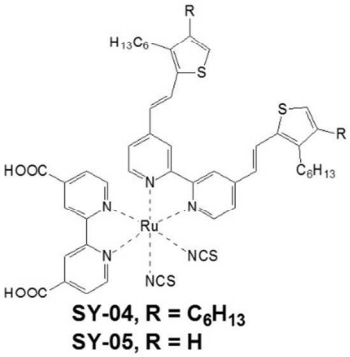

SY-04, R = C_6H_{13}
SY-05, R = H

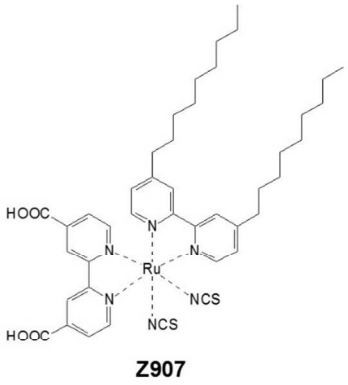

Z907